PHYSICS

DNS and scaling law analysis of compressible turbulent channel flow

LI Xinliang (李新亮)[1], MA Yanwen (马延文)[2] & FU Dexun (傅德薰)[1]

1. LNM, Institute of Mechanics, Chinese Academy of Sciences, Beijing 100080, China;
2. LHD, Institute of Mechanics, Chinese Academy of Sciences, Beijing 100080, China
Correspondence should be addressed to Li Xinliang (email: lixl@mail.tsinghua.edu.cn)

Received June 12, 2000

Abstract Fully developed compressible turbulent channel flow ($Ma = 0.8$, $Re = 3300$) is numerically simulated, and the data base of turbulence is established. The statistics such as density-weighted mean velocity and RMS velocity fluctuations in semi-local coordinates agree well with those from other DNS data. High order statistics (skewness and flatness factors) of velocity fluctuations of compressible turbulence are reported for the first time. Compressibility effects are also discussed. Pressure-dilatation absorbs part of the kinetic energy and makes the streaks of compressible channel flow more smooth. The scaling laws of compressible channel flow are also discussed. The conclusions are: (a) Scaling law is found in the center area of the channel. (b) In this area, ESS is also found. (c) When Mach number is not very high, compressibility has little effect on scaling exponents.

Keywords: **compressible turbulent flow, direct numerical simulation, high-order statistics, scaling law, streaks.**

Direct numerical simulation (DNS), as an important tool in turbulence research, simulates turbulent flows numerically by solving the Navier-Stokes equations directly. Because no model is used, DNS is very exact and universal, and it can provide information of the whole fluid, and it is very useful in the research of turbulence physics[1]. Since the 1980s, there have been many DNS data for solving the complex flow fields such as turbulent channel flow, turbulent mixing layer, turbulent boundary layer and turbulent jet, but most of them are incompressible, and DNS data of compressible turbulence are rather few. However, many engineering problems (such as problems associated with aeronautics and astronautics) are associated with compressible turbulence, so DNS of compressible turbulence is also very important.

Compressible turbulent channel flow is a typical flow because it contains wall boundary effects and compressibility effects. In this flow the boundary condition of the wall can be isothermal or adiabatic and they are different from each other. In this paper, we use isothermal-wall boundary condition.

Effects of compressibility can be categorized into two types: those associated with variations of the mean properties, and those due to fluctuations of thermodynamic quantities (so-called acoustic effects[2]). According to Morkovin's hypothesis, dominant compressibility effect is due to mean property when pressure fluctuation is much less than its mean value[3]. Bradshaw[4] and Spina et al.[5] found that only the mean effects are significant for transonic and supersonic wall-

bounded flows ($Ma < 5$). Coleman et al.[2] got the same conclusion from the DNS data of supersonic isothermal-wall channel turbulence with $Ma = 1.5$ and 3.

However, acoustic effects are not totally negligible. Coleman et al. found that the near-wall streaks become "less wiggly" as the Mach number increases and suggest it is an acoustic effect. Until now there is no clear conclusion on compressibility effects.

DNS of compressible turbulence has to solve the compressible N-S equations numerically. The compressible N-S equations are much more complicate than the incompressible ones. In the compressible N-S equations, viscous terms are also nonlinear as convection ones, and the continuous equation, the moment equation and the energy equation are coupled. Because the compressible N-S equations are much more difficult to solve, there are much fewer DNS results for compressible turbulence than for incompressible turbulence. Besides Coleman et al., L. Gamet et al. performed a DNS of compressible turbulent channel flow with $Ma = 0.2$. Because of the low Mach number, the characteristics of flow are very close to those of the incompressible ones.

In this paper, turbulent channel flow with isothermal-wall is numerically simulated by using upwind compact schemes on non-uniform meshes[6,7]. Data base of fully developed compressible turbulent flow is established. Mean profiles of streamwise velocity, pressure, temperature and density are provided. Mean dissipation rate of turbulent kinetic energy and Kolmogorov length scale are also discussed. The high-order statistics of velocity fluctuations are reported for the first time.

The density-weighted mean velocity (with Van Direst transformation) and RMS velocity fluctuations in semi-local coordinates agree well with those of Kim et al. and Coleman et al.

In this paper, compressibility effects on the near-wall streaks are discussed, and the difference between streaks of compressible and incompressible flows is studied through the analysis of spanwise two-point correlation of velocity fluctuations. According to this paper, pressure-dilation absorbs part of turbulent kinetic energy near the wall, which makes the streaks more smooth.

Scaling law is a hot topic in turbulence physics in recent years. It states that in the inertial-range scales, all moments of velocity fluctuations (so-called structure of velocity) at scale l have a power-law dependence on the scale l: $\langle |\delta u_l|^p \rangle \sim l^{\zeta_p}$. Scaling law plays an important role in turbulence physics and becomes one criterion for testing various theories of turbulence.

According to Kolmogorov's theory of 1941 (K41)[8] scaling exponent $\zeta_p = p/3$. However, the experimental data of high-order scaling exponents are substantially lower than the K41 prediction. This is the so-called anomalous scaling which becomes the greatest challenge to K41 theory. She et al. developed a hierarchical structure model (SL Model)[9,10], which predicts a nonlinear scaling exponent $\zeta_p = p/9 + 2\left(1 - \left(\frac{2}{3}\right)^p\right)$, and agrees well with experiments.

In recent years, DNS data have been successfully used in the study of scaling law of homogeneous turbulence, but there is no report about the DNS data used for the compressible turbulence. In this paper, DNS data are used in the scaling of the compressible turbulent channel flow for the first time, and the following conclusions are obtained: (a) Scaling law is found in the center area of channel. (b) In the same area, ESS is also found. (c) When Mach number is not very high, compressibility has little effect on scaling exponent.

1 Numerical procedure

Fig. 1 shows the two-dimensional counterpart of the three-dimensional flow geometry and co-

ordinate system. The flow is driven by a uniform body force. Temperature in two walls is the same and remains constant.

The non-dimensional compressible N-S equations are

$$\frac{\partial \boldsymbol{U}}{\partial t}+\frac{\partial \boldsymbol{E}}{\partial x}+\frac{\partial \boldsymbol{F}}{\partial y}+\frac{\partial \boldsymbol{G}}{\partial z}=\boldsymbol{P}+\frac{\partial \boldsymbol{E}_v}{\partial x}+\frac{\partial \boldsymbol{F}_v}{\partial y}+\frac{\partial \boldsymbol{G}_v}{\partial z},$$

where $\boldsymbol{U}=[\rho,\rho u,\rho v,\rho w,e]^{\mathrm{T}}$, $\boldsymbol{E},\boldsymbol{F},\boldsymbol{G},\boldsymbol{E}_v,\boldsymbol{F}_v,\boldsymbol{G}_v,\boldsymbol{P}$ are convection items, viscous items and body force, respectively.

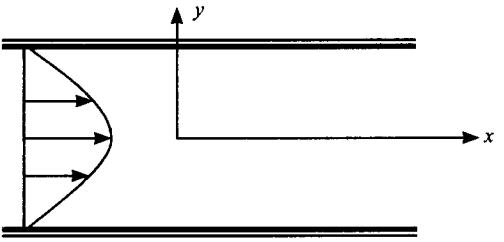

Fig. 1. The geometry and coordinate system of compressible channel flow.

The dynamic viscosity is a function of temperature, and the Sutherland's equation is used:

$$\frac{\mu}{\mu_0}=\left(\frac{T}{288.15}\right)^{1.5}\frac{288.15+C}{T+C},$$

where $C=110.4$. The non-dimensional numbers are defined as: $Re=\dfrac{U_mL}{\nu_0}$, $Ma=\dfrac{U_m}{c_0}$, where Re is the Reynolds number, Ma is the Mach number, U_m is the mean bulk velocity, L is the half-width of the channel, ν_0 is viscosity at the wall temperature, c_0 is sound speed at the wall temperature.

Periodic boundary conditions are used in the homogeneous streamwise and spanwise directions, while isothermal and no-slip boundary conditions are used on the wall[2].

Uniform streamwise and spanwise meshes and non-uniform meshes in cross-direction are used. The grid spaces are contracted near the wall.

The convection terms of the N-S equations are approximated by using up-wind compact difference schemes on non-uniform meshes[6,7], and the viscous terms are approximated by using symmetrical compact difference schemes on non-uniform meshes[11]. Third order R-K method is used in time-advancement. The body force is chosen to vary in time such that the total mess flux remains constant.

In order to compare the incompressible with the compressible flow, incompressible turbulent channel flow is also numerically simulated in this paper.

1.1 Computational conditions of compressible turbulent channel flow

The numerical parameters of compressible DNS are: $Ma=0.8$, $Re=3300$, $Pr=0.7$ (these parameters are non-dimensionalized by the mean bulk velocity, the sound speed and the viscosity at the wall temperature).

Computation domain is: $L_x=L_z=2\pi$, $L_y=2$, and computational meshes are $101\times140\times101$, x is the streamwise coordinate, z is the spanwise coordinate and y is the cross-direction coordinate. $y=\pm1$ are walls.

Computation is initialized as superimposing random velocity fluctuation (the amplitude of random velocity is 20% of the mean flow) upon a laminar parabolic velocity and computations were carried out on the SW-I super computer of Beijing High-Performance Computer Center. Parallel computing is carried out on 64 (or 32) CPUs, and it takes about 6s per time step (64 CPUs) or 10s (32 CPUs) per time step. Statistical equilibrium is reached after $t=100$, and results were then averaged over about 300 non-dimensional time unit.

1.2 Computational conditions of incompressible turbulent channel flow

The Reynolds number is 3300 for the incompressible turbulent flow (based on the mean bulk velocity and half-width of the channel). The computational domain is the same as for the compressible counterpart, and computational meshes are $64 \times 130 \times 64$.

The highly efficient method for the incompressible N-S equations in ref. [6] is used in computation, and it takes about 2s per time step (32 CPUs).

2 Statistics and analysis

Fig. 2(a),(b) are the mean profiles of compressible turbulent channel flow, where fig. 2 (a) shows the profiles of mean velocity non-dimensionalized by wall-shear velocity. In the figure the dashed lines are results of ref. [2] ($Ma = 1.5$) and ref. [6] ($Ma = 0$). It shows that the profile of $Ma = 0.8$ is in the middle between the profiles of $Ma = 1.5$ and $Ma = 0$. Fig. 2(b) shows the profiles of mean density, temperature and pressure. According to this figure, maximum temperature and minimum density are found at the center line and the mean flow is approximately isobaric. Near the wall there are great gradients of mean temperature and density and these are very important attribute of the isothermal wall flow[2].

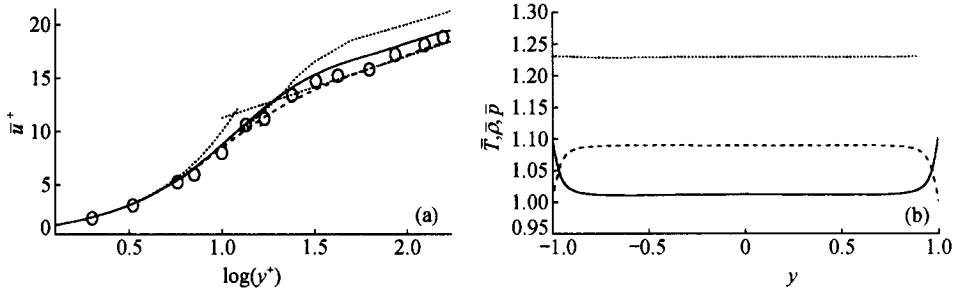

Fig. 2. (a) Mean streamwise velocity. ——, $Ma = 0.8$; ·····, $Ma = 1.5$; - - - -, $Ma = 0$; ○, experimental data of $Ma = 0$ (Kim et al.[12]). (b) Mean profiles of density, pressure and temperature. ——, Mean density; ·····, mean pressure; - - - -, mean temperature.

The Reynolds number based on the mean wall shear velocity is defined as $u_\tau = \sqrt{\frac{\tau_w}{\rho_w}}$, $Re_\tau = \frac{u_\tau L}{v}$, where $\tau_w = \mu_w \left.\frac{\partial \bar{u}}{\partial y}\right|_w$. In this paper, $u_\tau = 0.056$, $Re_\tau = 185$.

In our computation the Mach number is not very high, so according to Morkovin's theory, dominant compressible effects are due to mean property variations, especially the variations of mean-density. Coleman et al. studied the density-weighted mean velocity $\bar{u}^+_{VD}$ by using Van Driest transform[2,13]:

$$\bar{u}^+_{VD} = \int_0^{\bar{u}^+} \left(\frac{\bar{\rho}}{\rho_w}\right)^{1/2} \mathrm{d}\bar{u}^+.$$

Coleman et al.[2] found that $\bar{u}^+_{VD}$ of compressible flows ($Ma = 1.5$ and 3) are close to those of incompressible

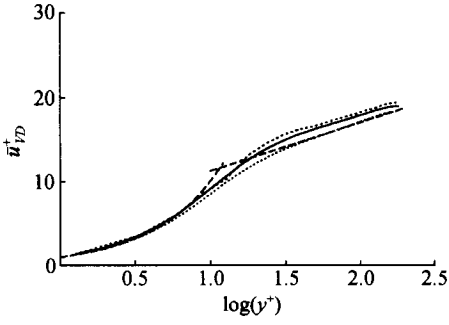

Fig. 3. Profiles of density-weighted mean velocity. ——, $Ma = 0.8$; ·····, $Ma = 0$; - - - -, $Ma = 1.5$; - - - - -, theory of $Ma = 0$ (wall-law and log-law).

flow.

Fig. 3 shows the profiles of $\bar{u}^+_{VD}$ for the flow with various Mach numbers, where solid line is for the profile with $Ma = 0.8$, dashed lines are $Ma = 0$ and $Ma = 1.5$. Three lines are very close.

Coleman et al. find that RMS velocity fluctuation profiles increase with Mach number, but when the "semi-local" scaling suggested by Huang et al. is used instead, the profiles of different Mach numbers are very close to each other. "Semi-local" scaling is defined as: $y^* = \tilde{y} u^*_\tau \bar{\rho}(y)/\bar{\mu}(y)$, where $u^*_\tau = \sqrt{\frac{\tau_w}{\bar{\rho}(y)}}$, $\tilde{y} = 1 - |y|$, and semi-local non-dimensionalized RMS velocity fluctuation are defined as

$$u'^*_{rms} = \frac{u'_{rms}}{u^*_\tau}, \quad v'^*_{rms} = \frac{v'_{rms}}{u^*_\tau}, \quad w'^*_{rms} = \frac{w'_{rms}}{u^*_\tau}.$$

Fig. 4 shows the profiles of semi-local non-dimensionalized RMS velocity fluctuation. According to this figure, profiles of $Ma = 0.8$, $Ma = 0$, $Ma = 1.5$ and $Ma = 3$ are very close, which validate the DNS data in this paper.

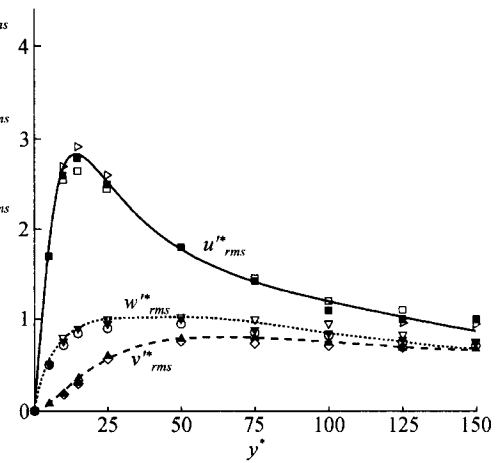

Fig. 4. RMS velocity fluctuation in "semilocal" coordinate.

The computed skewness and flatness factors of velocity fluctuation are shown in fig. 5(a),(b). Skewness and flatness factors are high-order statistics. The small asymmetry and oscillations in the profiles show the adequacy of the sample size. The skewness and flatness factors for compressible turbulent channel flow are reported for the first time.

Fig. 6 and fig. 7 show respectively the profiles of mean dissipation rate of turbulent kinetic energy $\bar{\varepsilon}^+$ and mean Kolmogorov length scale η^+_k, where $\bar{\varepsilon} = \nu \overline{\frac{\partial u'_i}{\partial x_j}\left(\frac{\partial u'_i}{\partial x_j} + \frac{\partial u'_j}{\partial x_i}\right)}$, $\eta_k = (\nu_3/\bar{\varepsilon})^{1/4}$, $\bar{\varepsilon}^+ = \bar{\varepsilon}\nu/u^4_\tau$, $\eta^+_k = \eta_k u_\tau/\nu$.

Solid lines are the results of this paper ($Ma = 0.8$) and symbols are the results of $Ma = 0.2$[11].

	u'^*_{rms}	v'^*_{rms}	w'^*_{rms}
$Ma = 0.8$	——	- - - -	·····
$Ma = 0$	□	△	▽
$Ma = 1.5$	■	▲	▼
$Ma = 3$	▷	◇	○

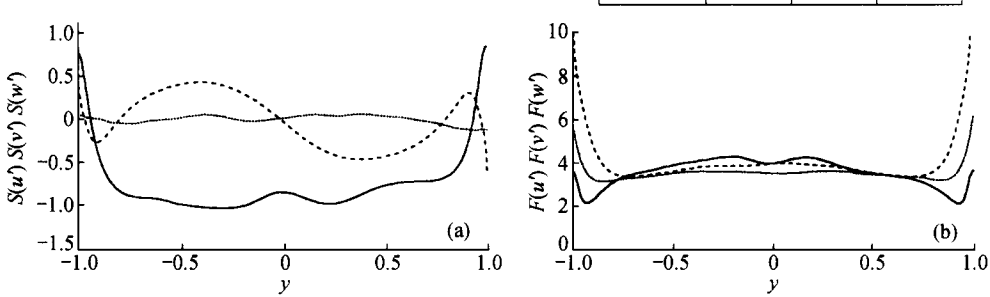

Fig. 5. (a) Skewness factor of velocity fluctuation ($Ma = 0.8$). ——, $S(u')$; - - - -, $S(v')$; ·····, $S(w')$. (b) Flatness factor of velocity fluctuation ($Ma = 0.8$). ——$F(u')$; - - - -, $F(v')$; ·····, $F(w')$.

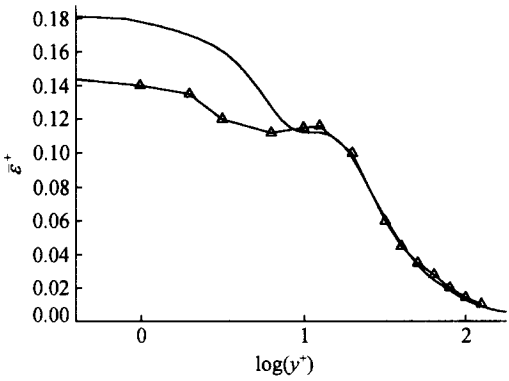

Fig. 6. Distribute of $\bar{\varepsilon}^+$ in wall coordinates. —, $Ma = 0.8$; △, $Ma = 0.2$.

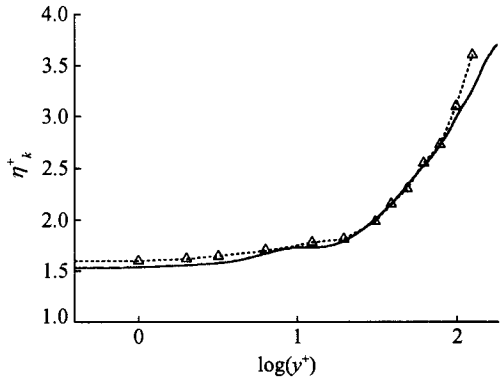

Fig. 7. Distribute of η_k^+ in wall coordinates. —, $Ma = 0.8$; △, $Ma = 0.2$.

It can be seen that the dissipation rate for $Ma = 0.8$ is a little higher than that for $Ma = 0.2$ (which can be considered as incompressible flow), and Komogorov scale for $Ma = 0.8$ is a little lower than that for $Ma = 0.2$.

Near-wall streaks are dominant feature of the wall-turbulence. Refs. [2, 12] studied the near-wall streaks of compressible and incompressible turbulent channel flow respectively. It is found that the streaks became more smooth as Mach number increases. Fig. 8(a) and (b) show distributions of streamwise velocity at $1 - |y| = 0.04$ for the flow of $Ma = 0.8$ and $Ma = 0$ respectively. It can be seen that the streaks of compressible flow is more smooth.

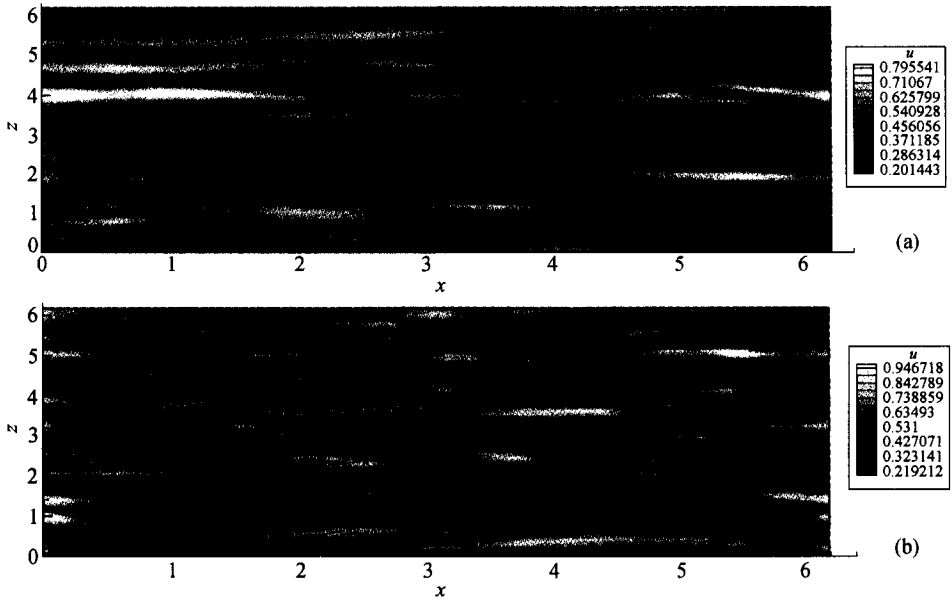

Fig. 8. (a) Instantaneous snapshots of stream velocity at $1 - |y| = 0.04$ ($Ma = 0.8$). (b) Instantaneous snapshots of stream velocity at $1 - |y| = 0.04$ ($Ma = 0$).

Fig. 9 shows the spanwise two-point correlation of the velocity fluctuation, which is defined as: $Ruu(z) = \overline{u'(x,y,z'+z)u'(x,y,z)} / \overline{u'^2(x,y,z')}$. The spanwise correlation shows that negative minima occur at $z = 0.311 (z^+ = 57.73)$, providing an estimate of the mean spac-

ing between the high- and low-speed fluid. It means that in our computation the mean spacing between the streaks should be 115.46, while the counterpart spacing of incompressible flow is 100 (in wall units)[11,12]. So the space between streaks of compressible flow is wider than that of incompressible flow.

In this paper, the terms associated with compressibility in energy equation are analyzed, and it is found that the pressure-dilated terms absorb part of turbulent kinetic energy, makes the near wall streaks more smooth.

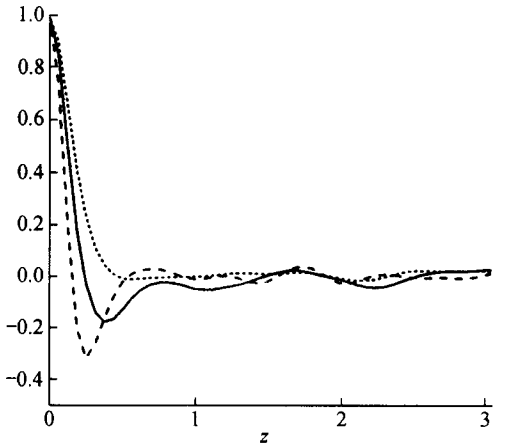

Fig. 9. Spanwise two-point correlation functions at $1-|y|=0.04$. ——, $Ruu(z)$; - - - -, $Rvv(z)$; ……, $Rww(z)$.

The energy equation is

$$\frac{\partial U}{\partial t}+u_j\frac{\partial U}{\partial x_j}=-\frac{p}{\rho}\frac{\partial u_j}{\partial x_j}-\frac{\mu}{Re\rho}\frac{2}{3}\delta_{ij}\frac{\partial u_l}{\partial x_l}\frac{\partial u_i}{\partial x_j}+\frac{\mu}{Re\rho}\left(\frac{\partial u_i}{\partial x_j}+\frac{\partial u_j}{\partial x_i}\right)\frac{\partial u_i}{\partial x_j}+\frac{C_p}{RePr\rho}\frac{\partial}{\partial x_j}\left(\mu\frac{\partial T}{\partial x_j}\right),$$

where $U=C_vT$ is inner-energy, $C_v=1/(\gamma(\gamma-1)Ma^2)$, $C_p=\gamma C_v$, $\gamma=1.4$.

The following two terms which absorb the kinetic and transfer it into inner-energy are associated with compressibility:

$$\varphi_1=-\frac{p}{\rho}\nabla\cdot V,\quad \varphi_2=-\frac{\mu}{Re\rho}\frac{2}{3}(\nabla\cdot V)^2.$$

In channel turbulence, $\bar{u}=\bar{u}(y)$, $\bar{v}=\bar{w}=0$. Divergence of mean velocity is zero, so $\nabla\cdot V$ is actually the divergence of velocity fluctuation, φ_1 and φ_2 are terms associated with the absorption of turbulent kinetic energy.

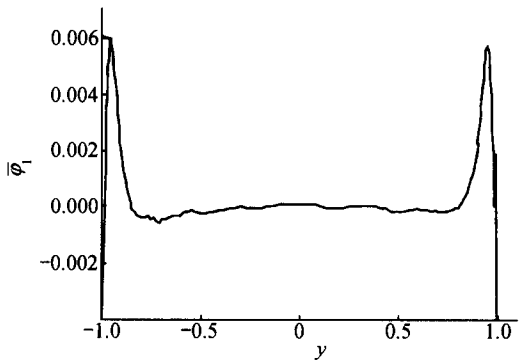

Fig. 10. Profile of $\bar{\varphi}_1$.

According to computational data, $\nabla\cdot V$ has the order of 1, so $\varphi_1:\varphi_2\sim 1:\frac{1}{Re}$, and φ_2 can be ignored since Reynolds number is high enough.

Fig. 10 shows the profile of $\bar{\varphi}_1$, in which there is a positive peak near the wall (about 0.006, this value is significant for the turbulent kinetic energy). The profile indicates that in the area near the wall, part of turbulent kinetic energy is absorbed and transferred into inner-energy. This makes the velocity streaks more smooth.

Fig. 11 shows the space distribution of φ_1 at $1-|y|=0.04$. In this figure, there are clear streak structures as in fig. 8, which validate the correlation between φ_1 and velocity streaks.

3 Analysis of the scaling law

Scaling law is a hot topic in turbulence physics in recent years, and DNS data have been successfully used in the study of scaling law of homogeneous turbulence, but there is no report

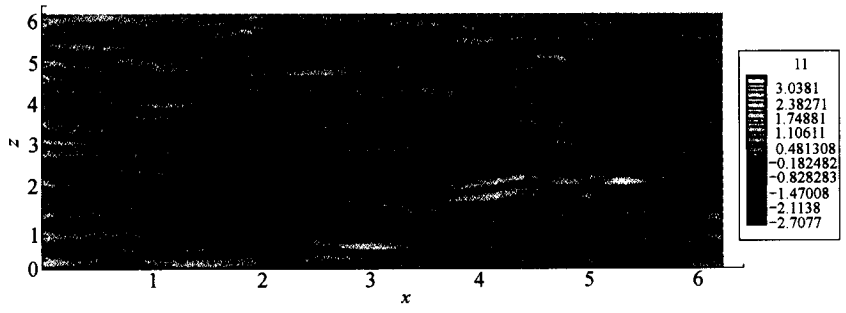

Fig. 11. Instantaneous snapshots of φ_1 at $1 - |y| = 0.04$.

about the DNS data used in the study of scaling law for the compressible turbulence. In this section, scaling laws for turbulent channel flow are studied basing on the DNS data.

Scaling law states that all moments of velocity fluctuations at scale l (so-called structure function of velocity) have a power-law dependence on the scale l in the inertial-range scales: $\langle |\delta u_l|^p \rangle \sim l^{\zeta_p}$, and ζ_p is called scaling exponent. Extended Self-Similarity (ESS) is one of the important developments in the measurement of scaling exponents[14]. It is developed by Benzi et al. and states that the velocity structure function of any order p depends on the structure function of order q (usually 3) in a much better power law: $\langle |\delta u_l|^p \rangle \sim \langle |\delta u_l|^q \rangle^{\zeta_{p,q}}$, $\zeta_{p,q}$ is called relative scaling exponent. ESS provides a new method for measuring scaling exponent with improved reliability.

Fig. 12(a) shows a plot of $\ln \langle |\delta u_l|^p \rangle$ as a function of $\ln l$ at the center of channel ($y = 0$ or $y^+ = 185$). From this figure it can be seen that all of those lines have linear range (the slope rate k in the figure equals the relative scaling exponents, it is reliable since ESS are used). This figure indicates the existence of scaling law in the turbulent flow in the center area of the channel.

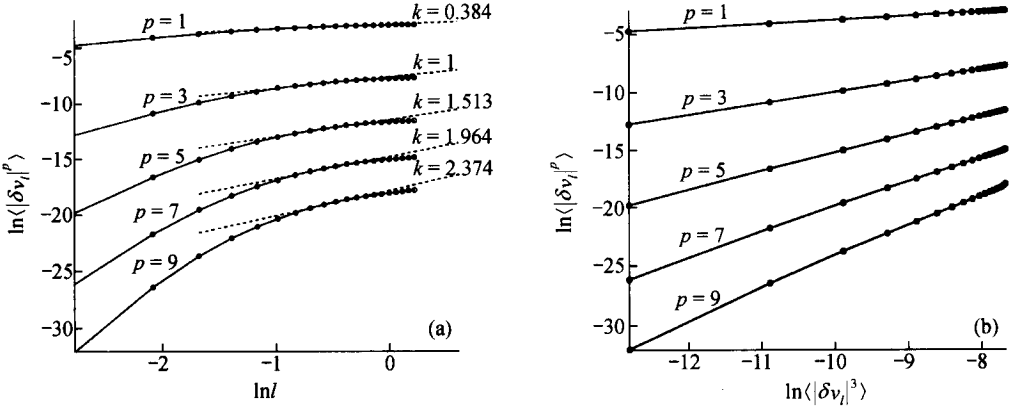

Fig. 12. (a) Profile of $\ln \langle |\delta v_l|^p \rangle$ as a function of $\ln l$ at location $y = 0$. (b) Profile of $\ln \langle |\delta v_l|^p \rangle$ as a function of $\ln \langle |\delta v_l|^3 \rangle$ at location $y = 0$.

Fig. 12(b) shows the plot of $\ln \langle |\delta u_l|^p \rangle$ as a function of $\ln \langle |\delta u_l|^3 \rangle$ in the turbulent flow at $y = 0$. For all p, $\ln \langle |\delta u_l|^p \rangle$ is shown as a strict linear function of $\ln \langle |\delta u_l|^3 \rangle$. This figure shows clearly the existence of ESS of the turbulent flow in the center liner of the channel.

Fig. 13(a),(b) show respectively $\ln\langle|\delta u_l|^p\rangle$ as a function of $\ln l$ and $\ln\langle|\delta u_l|^3\rangle$ at the location of $y^+ = 150$. It can be seen that scaling law and ESS also exist at $y^+ = 150$. Therefore the conclusion is: scaling law and ESS are found in the compressible turbulent flow in relatively wide range near the center of the channel.

Because of the relatively low Reynolds number, the inertial-range of turbulence cannot be very wide, so the linear-range in figs. 12(a) and 13(a) is relatively narrow for higher p.

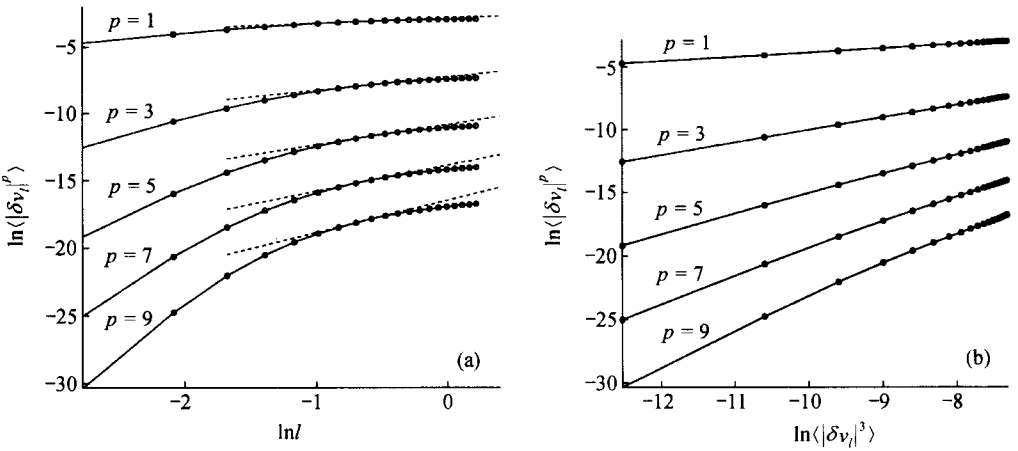

Fig. 13. (a) Profile of $\ln\langle|\delta v_l|^p\rangle$ as a function of $\ln l$ at location $y^+ = 150$. (b) Profile of $\ln\langle|\delta v_l|^p\rangle$ as a function of $\ln\langle|\delta v_l|^3\rangle$ at location $y^+ = 150$.

Fig. 14 shows the relative scaling exponent of the numerical results of this paper, those from experimental data, K41 theory and SL theory, where experimental data include: (a) wind tunnel turbulence (Anselmet et al.[15], $Re_\lambda = 515$ (based on Taylor microscale)); (b) weak turbulence (Benzi et al.[16], $Re_\lambda = 225$—800); (c) jet turbulence (Noullez et al.[17], $Re_\lambda = 365$—605, transverse velocity structure function); (d) DNS of isotropic turbulence (Cao et al. $Re_\lambda \approx 210$[18]). (a)—(d) are incompressible turbulence.

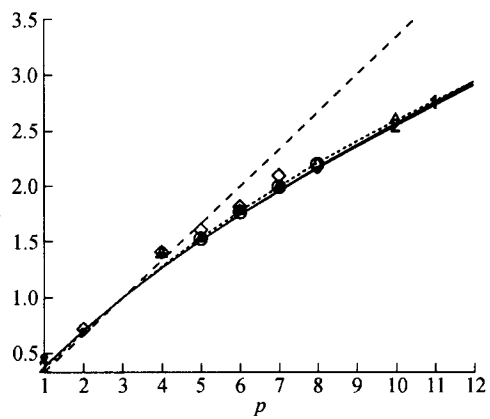

Fig. 14. Scaling exponents.

The result from DNS data of incompressible turbulence of this paper agrees well with those from experimental data (or other DNS data). It shows the exactness of the incompressible DNS data. It also can be seen that there is small difference between the scaling exponent from compressible and incompressible data, so we can draw the conclusion that compressibility has little effect on scaling exponent when the Mach number is not very high.

Fig. 14 shows that the DNS results agree very well with the predicted values by SL theory. It means that both results are believable.

4 Summary

Fully developed compressible turbulent channel flow ($Ma = 0.8$, $Re = 3300$) is simulated

by using upwind compact schemes on non-uniform meshes. The statistics such as density-weighted mean velocity and RMS velocity fluctuations in semi-local coordinates agree well with those from other DNS data.

Compressibility effects are also discussed. It is shown that the pressure-dilatation absorbs part of the kinetic energy and makes the streaks of compressible channel flow more smooth.

The scaling laws of compressible channel flow are also discussed. Scaling law and ESS are found in the center area of the channel, and when the Mach number is not very high, the compressibility has little effect on scaling exponents. The scaling exponent from the DNS data of this paper agrees well with those from the predicted value by SL theory, which means that both results are believable.

Acknowledgements The work was supported by NKBRSF (CG199032805), State Key Project and National Natural Science Foundation of China (Grant No. 19972070). Computation was performed on SW - I super computer of Beijing High Performance Computer Center and the computer group of State Key Lab. of Scientific and Engineering Computing. The authors would like to thank Prof. Zhang Linbo of LSSC and the experts of BHPCC for their help in programming and running computers.

References

1. Moin, P., Mahesh, K., Direct numerical simulation: A tool in turbulence research, Annu. Rev. Fluid. Mech., 1998, 30: 535.
2. Coleman, G. N., Kim, J., Moser, R. D., A numerical study of turbulent supersonic isothermal-wall channel flow, J. Fluid. Mech., 1995, 305: 159.
3. Morkovin, M. V., Effects of compressibility on turbulent flows, in Mechanique de la Turbulence (ed. Favre, A), New York: Gordon & Breach, 1964, 367—380.
4. Bradshaw, P., Compressible turbulent shear layers, Annu. Rev. Fluid Mech., 1977, 9: 33.
5. Spina, E. F., Smits, A. J., Robinson, S. K., The Physics of supersonic turbulent boundary layers, Annu. Rev. Fluid. Mech., 1994, 26: 287.
6. Li Xinliang, Ma Yanwen, Fu Dexun, DNS of incompressible turbulent channel flow with upwind compact scheme on non-uniform meshes, Computational Fluid Dynamics Journal, 2000, 8(4): 536.
7. Fu Dexun, Ma Yanwen, A high order accurate difference scheme for complex flow fields, J. Comput. Phys., 1997, 134: 1.
8. Kolmogorov, A. N., Local structure of turbulence in an incompressible viscous fluid at very high Reynolds numbers, Dokl Akad Nauk SSSR, 1941, 31: 538.
9. She, Z. S., Su, W. D., Hierarchical structures and scalings in turbulence, Advance in Mechanics (in Chinese), 1999, 29 (3): 289.
10. She, Z. S., Leveque, E., Universal scaling laws in fully developed turbulence, Phys. Rev. Lett., 1994, 72(3): 336.
11. Gamet, L., Dackos, F., Nicoud, F. et al., Compack finite difference schemes on non-uniform meshes Application to direct numerical simulations of compressible flows, Int. J. Numer. Meth. Fluids, 1999, 29: 159.
12. Kim, J., Moin, P., Moser, R., Turbulence statistics in fully developed channel flow at low Reynolds number, J. Fluid. Mech., 1987, 177: 133.
13. Huang, P. G., Coleman, G. N., Bradshaw, P., Compressible turbulent channel flows: DNS results and modeling, J. Fluid Mech., 1995, 305: 185.
14. Benzi, R., Ciliberto, S., Ruiz Chavarria, G. et al., Extended self-similarity in the dissipation range of fully developed turbulence, Europhys. Lett., 1993,24(4): 275.
15. Anselmet, F., Gagne, Y., Hopfinger, E. J., High order velocity structure functions in turbulent shear flows, J. Fluid Mech., 1984, 140: 63.
16. Benzi, R., Ciliberto, S., Baudet, C. et al., On the intermittent energy transfer at viscous turbulence, Physica D, 1995, 80 (4): 385.
17. Noullez, A., Wallace, G., Lempert, W. et al., Transverse velocity increments in turbulent flow using the relief technique, J. Fluid Mech., 1997, 339: 287.
18. Cao, N. Z., Chen, S. Y., She, Z. S., Scalings and relative scalings in the Navier-Stokes turbulence, Phys. Rev. Lett., 1996, 76(20): 3711.